



## Scaling relations in rheology of concentrated starches and maltodextrins

Ruud van Der Sman, Job Ubbink, Marina Dupas-Langlet, Magdalena Kristiawan, Isabel Siemons

### ► To cite this version:

Ruud van Der Sman, Job Ubbink, Marina Dupas-Langlet, Magdalena Kristiawan, Isabel Siemons. Scaling relations in rheology of concentrated starches and maltodextrins. Food Hydrocolloids, 2022, Food Hydrocolloids, 124 (Part B), pp.107306. 10.1016/j.foodhyd.2021.107306 . hal-03330859

**HAL Id: hal-03330859**

**<https://hal.inrae.fr/hal-03330859>**

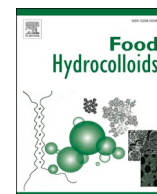
Submitted on 14 Dec 2021

**HAL** is a multi-disciplinary open access archive for the deposit and dissemination of scientific research documents, whether they are published or not. The documents may come from teaching and research institutions in France or abroad, or from public or private research centers.

L'archive ouverte pluridisciplinaire **HAL**, est destinée au dépôt et à la diffusion de documents scientifiques de niveau recherche, publiés ou non, émanant des établissements d'enseignement et de recherche français ou étrangers, des laboratoires publics ou privés.



Distributed under a Creative Commons Attribution 4.0 International License



# Scaling relations in rheology of concentrated starches and maltodextrins

R.G.M. van der Sman<sup>a,b,\*</sup>, Job Ubbink<sup>c</sup>, Marina Dupas-Langlet<sup>d</sup>, Magdalena Kristiawan<sup>e</sup>, Isabel Siemons<sup>a</sup>

<sup>a</sup> Wageningen Food & Biobased Research, Wageningen University and Research, the Netherlands

<sup>b</sup> Food Process Engineering, Wageningen University and Research, the Netherlands

<sup>c</sup> Univ. Minnesota, United States

<sup>d</sup> Nestle Research Lausanne, Switzerland

<sup>e</sup> INRA Nantes, France

## ARTICLE INFO

### Keywords:

Rheology  
Superposition  
Glass transition  
Starch  
Maltodextrin

## ABSTRACT

Using literature data we have studied the rheological behaviour of concentrated maltodextrins and starches. We show that much of their rheology, like zero shear viscosity and shear thinning behaviour, appears to be governed by the ratio of the glass transition temperature and actual temperature,  $T_g/T$ , as the scaling parameter. Via this scaling, we can apply time-temperature-solvent superposition principle, which is also validated for linear dynamic viscoelastic experiments at different temperatures, compositions, and moisture content. Furthermore, we show that the dynamic viscoelastic experiments follow the Marin-Graessley model, indicating that concentrated maltodextrins and starches behave as transient (entangled) networks.

## 1. Introduction

Knowledge of the rheology of concentrated polysaccharides is important for quite a number of food and pharmaceutical processes: expansion of starchy snacks (Kristiawan et al., 2019; Philipp et al., 2018; van der Sman & Broeze, 2014); extrusion of breakfast cereals (Lai & Kokini, 1991); 3D printing (Gholamipour-Shirazi et al., 2019; Liu et al., 2019); spray drying (Palzer, 2009; Siemons et al., 2020), hot melt extrusion (Aho et al., 2015; Paradkar et al., 2009) and powder stability (Sritham & Gunasekaran, 2017; Ubbink & Dupas-Langlet, 2020). In these applications rheology is important for a) flow through constrictions like feeding nozzles or dies, b) sintering/agglomeration of multiple droplets or threads, or c) resistance of the food matrix against the expansion of bubbles or cavities. Hence, these different applications can benefit from a more general molecular and mechanistic description of the rheology of the polysaccharides present in the food matrices. In these applications often maltodextrins and starch are used as the food matrix. Maltodextrins are often used as model systems for understanding complex food processing like spray drying (Descamps et al., 2013; Gianfrancesco et al., 2010), powder stability and encapsulation (Dupas-Langlet et al., 2019; Ubbink, 2016; Ubbink & Dupas-Langlet, 2020).

As we have found for the zero-shear viscosity of a multitude of

carbohydrates (van der Sman & Mauer, 2019), we shall investigate whether the rheology of concentrated maltodextrins and starches is also governed by the scaling parameter  $T_g/T$ , which is the ratio of the glass transition temperature  $T_g$  and the actual temperature  $T$ , both given in Kelvin.

Also, for several synthetic polymers, a universal scaling of zero shear viscosity and structural relaxation times with  $T_g/T$  is claimed (Agapov et al., 2018; Ding & Sokolov, 2006; Liu et al., 2006; Maranas, 2007; Sokolov & Schweizer, 2009; Zorn et al., 1995). The original idea comes from Angell, who has used the scaling of viscosity with  $T_g/T$  to investigate the so-called fragility of systems (Angell, 2002), which is the relative strength of property changes in going from the liquid state to the glassy state (Zorn et al., 1995). Furthermore, recently it is shown that rheology of glycerol/water mixtures scales with  $T_g/T$  (Jensen et al., 2018). In food science, it is shown that horizontal shift factors for different soy pastes (differing in crosslink density) also follow the  $T_g/T$  scaling (Ashokan & Kokini, 2005).

We note, that in food science zero shear viscosity has often been modelled with Williams-Landel-Ferry (WLF) or Vogel-Fulcher-Tammann (VFT) theories. In particular, these theories have been applied to maltodextrins and starches (Avaltroni et al., 2004; Both et al., 2019; Normand et al., 2019; Sillick & Gregson, 2009; Ubbink & Dupas-Langlet, 2020). However, often model parameters have to be

\* Corresponding author. Wageningen Food & Biobased Research, Wageningen University and Research, the Netherlands.

E-mail address: [ruud.vandersman@wur.nl](mailto:ruud.vandersman@wur.nl) (R.G.M. van der Sman).

refitted for each moisture content, no universal values of these parameter apply for the whole or broad moisture content range. Moreover, it is suggested that the moisture dependent  $T_0$  parameter in the VFT theory is linear with  $T_g$  (Sillick & Gregson, 2009). If that assumption is inserted in the VFT theory, it would say that viscosity is a function of  $T_g/T$ . If this scaling of viscosity holds true for food materials, it will greatly improve their predictability as the model parameter  $T_g$  can be measured independently of rheology, in contrast to model parameters of WLF and VFT theory, which have to be fitted for each moisture content.

For many of the above-mentioned food applications actually the shear-rate dependent viscosity is more relevant for processing than the zero-shear viscosity (Della Valle et al., 1996; Gholamipour-Shirazi et al., 2019). Hence, we will first investigate the scaling of the shear-rate-dependent viscosity of maltodextrins and starch. Given the validity of the Cox-Merz rule for maltodextrins (Dupas-Langlet et al., 2019; Sillick & Gregson, 2009) the shear-rate dependent viscosity can also be obtained via dynamic viscoelastic experiments, i.e. small amplitude oscillatory (SAOS) rheology. Moreover, SAOS also renders information about the elastic part of the (linear) rheological response. For SAOS one often constructs master curves via the time-temperature superposition principle (Kristiawan et al., 2016). We question whether such time-temperature superposition can be extended to time-moisture-temperature superposition, using the  $T_g/T$  scaling parameter.

In this paper, we shall investigate in particular whether the various rheological properties of maltodextrins (Dupas-Langlet et al., 2019; Kasapis & Shrinivas, 2010) and (extruded) starch (Kasapis et al., 2000; Kristiawan et al., 2016) scale with  $T_g/T$ , and if this generalized superposition principle applies to zero shear viscosity, flow curves and SAOS measurements. If this scaling holds true, it would allow us to predict their rheological properties under conditions which are difficult to attain experimentally, but which are often very relevant for applications (Gholamipour-Shirazi et al., 2019; Kristiawan et al., 2019; Lai & Kokini, 1991; Liu et al., 2019; Palzer, 2009; Philipp et al., 2018; Siemons et al., 2020; van der Sman & Broeze, 2014).

The paper is organized as follows: first, we describe the theory for the shear-rate dependent viscosity, and the Marin/Graessley model. Subsequently, we present the results: a) the zero-shear viscosity of maltodextrins, b) the shear-rate dependent viscosity of maltodextrin and starches, and c) the SAOS rheology of maltodextrin and starch. We finalize with an overall discussion and conclusions.

## 2. Theory on rheology of concentrated polysaccharides

In this section we introduce theories describing the rheology of concentrated food biopolymers, in the regime of a) very large strains, and b) small oscillatory strains. Rheology in regime a) is normally obtained via measuring flow curves, showing the viscosity as a function of shear rate. Many biopolymers will show shear-thinning behaviour, where the viscosity decreases with shear-rate via a power law. In regime b) SAOS measurements will deliver both the viscous and elastic (linear) response of the material. In this paper, we restrict our investigations to concentrated food biopolymer solutions, where the concentration is significantly larger than the so-called overlap concentration  $c^*$ , which demarks the so-called semi-dilute regime. For even higher concentrations, in the so-called concentrated regime, the biopolymers are highly entangled and exhibit viscoelastic behaviour (Morris et al., 1981).

Shear-thinning happens due to the disentanglement of the polymer network: the transient network junctions are broken at a higher rate than they are created (Morris et al., 1981). In the shear-thinning regime the shear-rate dependent viscosity is often described as a power law:

$$\eta(\dot{\gamma}) = K_0 \dot{\gamma}^{n-1} \quad (1)$$

$K_0$  is the consistency, and  $n$  is the shear-thinning exponent.

Della Valle has proposed scaling for shear-thinning viscosity to

obtain a master curve (Kristiawan et al., 2016; Valle et al., 2007):

$$\eta/a_T = f(\dot{\gamma}a_T) \quad (2)$$

with  $a_T$  designated as the horizontal shift factor, which is later also used in the scaling of SAOS measurements.  $a_T$  has an Arrhenius-like dependency on temperature, but it is also dependent on moisture content. Only empirical correlations between  $a_T$  and moisture content have been developed. (Cervone & Harper, 1978; Kristiawan et al., 2016; Valle et al., 2007; Vergnes & Villemare, 1987). If the scaling is substituted into the above power-law relation, Eq. (1), we obtain:

$$\eta/a_T = K_{ref}(\dot{\gamma}a_T)^{n-1} \quad (3)$$

Here  $K_{ref}$  is the consistency at the reference temperature, where  $a_T = 1$ . The above relation implies that  $n$  is independent of the water content and temperature (Vergnes & Villemare, 1987).

Shear-thinning happens only beyond a critical shear rate  $\dot{\gamma}_{cr}$ . Below this critical value, one expects Newtonian behaviour of the viscosity. The Carreau-Yasuda model captures both Newtonian and shear-thinning behaviour: (Caputo et al., 2004; Fatkullin et al., 2011):

$$\eta(\dot{\gamma}) = \eta_0 [1 + (\dot{\gamma}/\dot{\gamma}_{cr})^a]^{(n-1)/a} \quad (4)$$

with  $n$  the same exponent as in the power law model, and  $\eta_0$  is the zero-shear viscosity. For entangled polymers it is found that  $0.2 < n < 0.4$ . The Carreau model assumes that  $a = 2$ , while the Cross model assumes that  $a = 1$ . For the general case it holds  $1 \leq a \leq 2$  (Heo & Larson, 2005). The inverse of the critical shear rate represents a fundamental relaxation time,  $\tau_{cr} = 1/\dot{\gamma}_{cr}$ , which is dependent on both temperature and moisture content (Caputo et al., 2004). Furthermore, for linear polymers it is found that  $\tau_{cr}$  depends on the molar weight:  $\tau_{cr} \sim M_w^p$ , leading to  $n = 1/p$  (Fatkullin et al., 2011). It is found that  $p \approx 3.5$ , and hence  $n \approx 0.3$  (Fatkullin et al., 2011; Stadler & Mahmoudi, 2011), agrees with most of the scalings found for food biopolymers (Bengochea et al., 2007; Redl, Morel, Bonicel, Guilbert, & Vergnes, 1999; Song et al., 2007; Valle et al., 2007).

It is assumed that both the zero-shear viscosity  $\eta_0$  and the relaxation time  $\tau_{cr}$  show an identical dependency on temperature and moisture. Hence, the Carreau-Yasuda model scales as:

$$\eta(\dot{\gamma}) = a_T \eta_{ref} [1 + (a_T \tau_{ref} \dot{\gamma})^a]^{(n-1)/a} \quad (5)$$

The Arrhenius function (Mighri et al., 2001) or WLF function is often applied for  $a_T$  (Aho & Syrjälä, 2008; Williams et al., 1955).

However, we pose the hypothesis, that similar to low molecular weight carbohydrates (van der Sman & Mauer, 2019), the zero-shear viscosity of food biopolymers can be modelled as a function of  $T_g/T$ , with  $T_g$  the glass transition temperature (Ubbink & Dupas-Langlet, 2020). This ratio captures both the effect of temperature  $T$  and the moisture content, as  $T_g$  is dependent on moisture, cf. the Couchman-Karasz model (Van der Sman & Meinders, 2011):

$$T_g = \frac{y_w T_{g,w} \Delta C_{p,w} + y_s T_{g,s} \Delta C_{p,s}}{y_w \Delta C_{p,w} + y_s \Delta C_{p,s}} \quad (6)$$

with  $y_w = 1 - y_s$  the mass fraction of water. In an earlier publication, we have shown that the Couchman-Karasz model holds for both starch and maltodextrins with the following parameter values:  $T_{g,w} = 134$  K for the glass transition of pure water,  $T_{g,s} = 500$  K for the glass transition of pure (dry) starch,  $\Delta C_{p,s} = 0.42$  J/kg.K, and  $\Delta C_{p,w} = 1.94$  J/kg.K the changes in heat capacity during the glass transition of the dry polysaccharide and water (Van der Sman & Meinders, 2011).

We expect the spectrum of the SAOS rheology to follow the universal master curve for associative networks/entangled polymers (Groot & Agterof, 1995), which is reproduced in Fig. 1. This universal master curve has four zones:

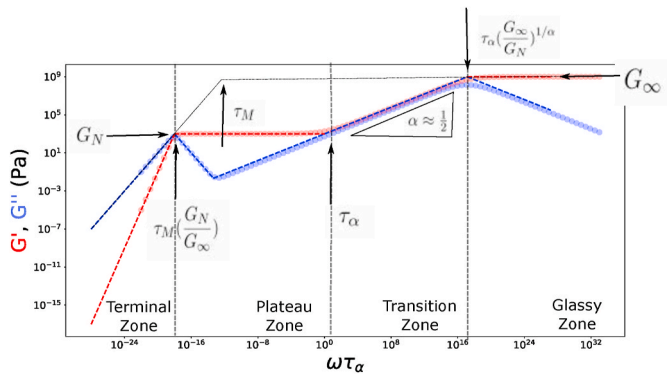


**Fig. 1.** Universal master curve for associative (transient) polymer networks, inspired by the graph in (Groot & Agterof, 1995), reproduced with the Marin-Graessley model. Also, we have indicated how characteristic points relate to model parameters.

- terminal zone
- plateau zone
- transition zone
- glassy zone

The graph shows the elastic modulus  $G'$  and the loss modulus  $G''$  as a function of the angular frequency  $\omega$ . In the terminal zone, the system behaves as a (creeping) viscous fluid, with  $G'' \sim \omega$  and  $G' \sim \omega^2$ , as follows from the Maxwell model of viscoelastic fluids. In the plateau zone, the system behaves more like a gel, with  $G' \gg G''$ . A characteristic point is the plateau value of  $G' = G_N$ , which appears if  $G''$  goes through a minimum.  $G_N$  is viewed as a measure of the crosslinks density, which can be either covalent or transient physical links like entanglements. In some systems, like oligomers with chains that are too short to entangle, the plateau zone can be even absent.

In the transient zone,  $G'$  and  $G''$  are of the same order. For long linear polymers, the Rouse model predicts a scaling with  $G' \sim G'' \sim \omega^{1/2}$ . For other polymer architectures, other scaling exponents are found. In this zone, the system behaves more like a (viscoelastic) liquid than in the plateau zone. At very short time scales the system behaves as a glassy system, showing a maximal value in  $G' = G_\infty$ . The maximum in  $G''$  is shown at the transition into the glassy state.  $G''$  decreases with frequency, with  $G' \gg G''$ : the glassy polymer responds as a hard elastic solid.

The Marin-Graessley model captures the essential aspects of the universal master curve in a quantitative way (Marin & Graessley, 1977). It supposes that the mechanical spectrum is the resultant of three relaxation modes, with one being the Maxwell relaxation, and another being the  $\alpha$ -relaxation, which is thought to occur universally in glass-forming systems. The  $\alpha$ -relaxation and the third relaxation mode are described by a Cole-Cole model, commonly used to describe dielectric properties of polymers.

The Marin-Graessley model is expressed in terms of the complex compliance  $J^* = 1/G^*$ , which is the inverse of the complex modulus:  $G^* = G' + iG''$  (with  $i = \sqrt{-1}$ ):

$$J^*(\omega) = J_\infty \left[ 1 + \frac{1}{i\omega\tau_M} + \frac{k_p}{1 + (i\omega\tau_p)^p} + \frac{k_\alpha}{1 + (i\omega\tau_\alpha)^\alpha} \right] \quad (7)$$

The third mode is included by Marin and Graessley to broaden and flatten the response in the plateau-zone, which can be due to polydispersity in the molecular weight distribution (Wasserman & Graessley, 1992).

We will also use a simplified (2-mode) model, having only the Maxwell and  $\alpha$ -relaxation modes:

$$J^*(\omega) = J_\infty \left[ 1 + \frac{1}{i\omega\tau_M} + \frac{k_\alpha}{1 + (i\omega\tau_\alpha)^\alpha} \right] \quad (8)$$

$\tau_M$  is the relaxation time of the Maxwell relaxation mode, and  $\tau_\alpha$  is the  $\alpha$  relaxation time.  $G_\infty = 1/J_\infty$  is the elastic modulus in the glassy zone, expected to be in the range of 1–10 GPa (Kilburn et al., 2005). The plateau modulus is related to  $G_N \approx k_a/J_\infty$ . The meaning of the various parameters is illustrated in Fig. 1.

If time-temperature superposition holds, all relaxation times  $\tau_M$ ,  $\tau_\alpha$ , and  $\tau_p$  should scale in a similar way as the zero shear viscosity  $\eta_0$  (Marin & Graessley, 1977). For maltodextrins it is assumed that the horizontal shift factor  $a_T$  indeed scales with the zero-shear viscosity (Dupas-Langlet et al., 2019; Palzer, 2010) - both following WLF theory for example (Williams et al., 1955).

### 3. Results

#### 3.1. Zero shear rheology of maltodextrins

For the zero-shear viscosity of carbohydrates,  $\eta_0$ , we have shown that a universal master curve is obtained if the viscosity is plotted against  $T_g/T$  (van der Sman & Mauer, 2019). We investigate whether that a similar master curve can also be obtained for maltodextrins that are characterized by relatively long chain lengths, i.e. maltodextrins of low dextrose equivalent ( $DE = 2$ ). Experimental data are obtained from the following data sources (Sillick & Gregson, 2009; Dupas-Langlet et al., 2019; Normand et al., 2019). In these studies the actual values of  $T_g$  of the measured mixtures are not given, but they have been fitted with either Gordon-Taylor or Couchman-Karas. In line with our previous studies, we have chosen to use Couchman-Karas, Eq. (6), for computing  $T_g$  for a given the moisture content  $y_w$ . For  $T_{g,s}$  of the dry material we use the values as given by the literature sources. For the other model parameters in Eq. (6) we take well established values, as indicated in several studies (D'Haene & Van Liederkerke, 1996; Van der Sman & Meinders, 2011; Normand et al., 2019; Siemons et al., 2020). Furthermore, we note that the use of predicted  $T_g$  values, as based on Couchman-Karas, has the advantage of averaging out unavoidable statistical fluctuations in the experimental values, and thus increases the accuracy of the constructed master curve. We note, that in the remainder of this paper the use of  $T_g$  also implies their predicted values using Couchman-Karas.

Thus, via the above procedure we construct the master curve without any parameter fitting. The constructed master curve for maltodextrins is shown in Fig. 2, together with the master curve for carbohydrates. We observe that the viscosity of maltodextrins of low DE values also shows a master curve if plotted against  $T_g/T$ , albeit that at high  $T_g/T$  values there is some deviations occurring. These deviations we attribute to difficulties with obtaining reliable experimental data at these very high viscosities, which have been obtained with a different experimental method than the data in the range  $T_g/T < 0.9$ . In this latter range the data of the different sources nicely superimpose on each other.

However, the resulting master curve of maltodextrins does not coincide with that of small sugars. Yet, the shape of both master curves is similar: the dashed line indicating the master curve of maltodextrin is fitted via vertical shifting of the carbohydrate master curve by a factor of 10. Angell states that viscosity curves of different compounds can have different master curves if plotted against  $T_g/T$  if they differ in fragility (Angell, 2002).

Several other data sets are comprising maltodextrin mixed with a small carbohydrate, namely maltopolymers mixed with maltose (Dupas-Langlet et al., 2019), and maltodextrin DE18 and sucrose (Sillick & Gregson, 2009). For these datasets we have also investigated, whether they follow the above scaling of zero shear viscosity with  $T_g/T$ . For these ternary mixtures, a modified Couchman-Karas relation needs to be used, to account for non-ideal mixing in the ternary mixture (van der



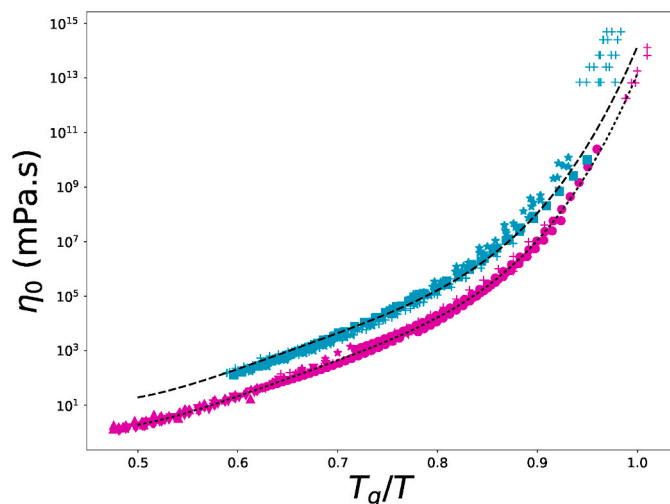


**Fig. 2.** Viscosity of simple carbohydrates and maltopolymers as function of  $T_g/T$ . Master curves for sugars and maltopolymer are indicated with solid and dashed lines respectively. Maltodextrins with low DE values collapse to a master curve (cyan symbols), which is significantly higher than those for simple sugars or polyols (magenta). Sources of experimental data and corresponding  $T_{g,s}$  values are indicated in Table 1, using the color coding of Matlab plots as listed in the table. (For interpretation of the references to color in this figure legend, the reader is referred to the Web version of this article.)

Sman, 2013; van der Sman & Meinders, 2013). Earlier, we have shown that the glass transition of dry mixtures of a biopolymer and a disaccharide does not follow the common Couchman-Karasch relation (van der Sman, 2013; van der Sman & Meinders, 2013), which is assumed to be due to large heterogeneity in the matrix, or even possible phase separation in the system - as hinted by recent measurements (Hughes et al., 2018; Martini et al., 2020; Masavang et al., 2019; Roudaut & Wallecan, 2015). We have accounted for this deviation via a weighted averaging of the  $T_g$  of the dry ingredients (van der Sman & Meinders, 2013). We have used the following relation, which is similar to the Gordon-Taylor equation:

$$T_{g,s} = \frac{y_{MDX} T_{g,MDX} + f(1 - y_{MDX}) T_{g,c}}{y_{MDX} + f(1 - y_{MDX})} \quad (9)$$

$y_{MDX}$  is the mass fraction of maltodextrin, and  $T_{g,c}$  is the glass transition temperature of the dry carbohydrate, i.e. either maltose or sucrose.  $f$  is a correction factor for the non-ideal mixing, which varies in the range  $2 \leq f \leq 6$  for disaccharides (van der Sman & Meinders, 2013). This non-ideal mixing is observed for several ternary mixtures of biopolymers, saccharides and water (Imamura et al., 2002; Shamblyn et al., 1996; Shamblyn & Zografis, 1998; Taylor & Zografis, 1998; Townrow et al., 2007; Vasanthavada et al., 2004). The cause of this deviation is the heterogeneity of the matrix of biopolymer and saccharide (Shamblyn & Zografis, 1998), similar as we have proposed for mixtures of starch, polyols and water (Van der Sman, 2019).

We apply this equation for characterizing the glass transition of dry mixtures of maltopolymer and maltose, and fit  $f$  to experimental data from (Dupas-Langlet et al., 2019; Ubbink et al., 2007). We note that the experimental data for  $T_g$  are obtained independently of the rheological data.

For the fitting we use the value of  $T_{g,c} = 353$  K for maltose,  $T_{g,c} = 336$  K for sucrose (van der Sman & Mauer, 2019), and  $T_{g,MDX} = 500$  K (Van der Sman & Meinders, 2011) for a long-chain maltodextrin. A reasonable fit is obtained for  $f = 5$ , as shown in Fig. B1 (see Supplementary Materials). Using the above equation,  $T_{g,s}$  is substituted in Eq. (6) to obtain  $T_g$  of the ternary mixture, which is then used for constructing the curve of zero shear viscosity  $\eta_0$  versus  $T_g/T$ . For the maltopolymer/maltose mixtures the scaling of  $\eta_0$  with  $T_g/T$  is shown in Fig. 3,

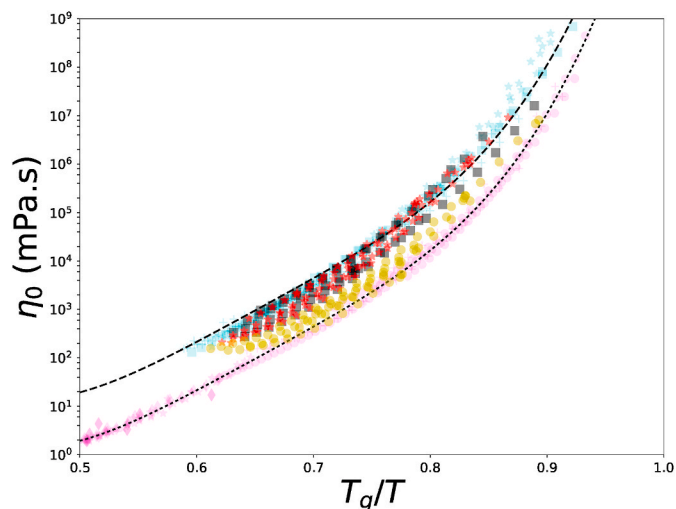


**Fig. 3.** Viscosity of maltodextrins, and mixtures of maltopolymer and maltose as function of  $T_g/T$ . The data falls in either of the two classes shown in Fig. 2. Sources of experimental data are indicated in Table 1, using the color coding of Matlab plots as listed in the table. (For interpretation of the references to color in this figure legend, the reader is referred to the Web version of this article.)

where we have used the rheological data of (Dupas-Langlet et al., 2019). This dataset also includes viscosity data in the range of  $0.9 < T_g/T < 1$ , but there is too much scatter in the data to draw any definite conclusions (as also shown in Fig. 2), and hence we have excluded these from Fig. 3.

In Fig. 3 we observe that the data sets for maltopolymer/maltose mixtures fall either in between the master curves (reproduced from Fig. 2), or on the master curve for large maltodextrins. The mixtures of maltopolymers and maltose show that 80:20 mixture (black squares = ks) and 50:50 mixture (red stars = r\*) follow largely the viscosity of the long-chain maltodextrins, while the 20:80 mixture (yellow circles = yo) is closer to the viscosity of the small carbohydrates.

We have also included new data recently measured in our lab on maltodextrins varying in DE-values (Siemons et al., 2020). These systems can be viewed as a polydisperse mixture of maltopolymers and small oligosaccharides/sugars, thus bearing a strong resemblance to the above bidisperse maltopolymer/sugar systems.  $T_g$  values are computed independently, using the relations established in our earlier paper (Siemons et al., 2020), where we combined Couchman-Karasch with the Fox-Flory relation. The latter relates  $T_{g,s}$  to the molecular weight of the maltodextrin (or equivalently the DE-value).

The viscosity versus  $T_g/T$  of the polydisperse maltodextrins is depicted in Fig. 4, with used symbols listed in Table 1 (following the coding of Matlab plot function). The used glass transition temperature of the dry ingredients  $T_{g,s}$  to compute  $T_g$  in the scaling parameter  $T_g/T$  is also listed in Table 1.

Despite some experimental variations, we observe that the data for the polydisperse maltodextrins largely fall on either the master curve for small sugars or the master curve for large maltodextrins. The datasets of DE5 and DE12 coincide with that of the larger maltodextrins, while for  $DE \geq 21$  the viscosity follows that of small sugars. Despite the clear variation in the experimental data, the results for the polydisperse maltodextrins also suggest that viscosity master curves fall in two distinct classes, as also shown in Fig. 2.

### 3.2. Shear thinning behaviour

Shear-thinning is observed for maltodextrin (18 DE) containing 16% water (Sillick & Gregson, 2009), including a Newtonian plateau of smaller shear rates. After rescaling the actual viscosity with zero-shear viscosity,  $\eta/\eta_0$ , and multiplication of the shear rate with  $\eta_0/\eta_{ref}$  a master flow curve can be constructed using measurements at various

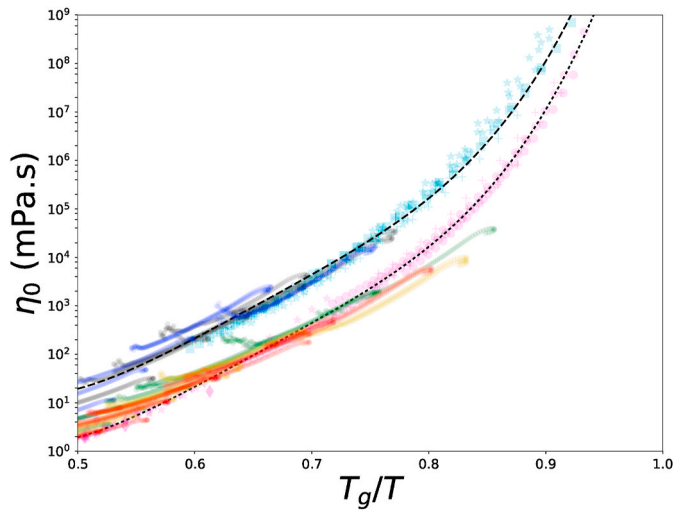


**Fig. 4.** Viscosity of polydisperse maltodextrins as function of  $T_g/T$ . The data falls in either of the two classes shown in Fig. 2. Sources of experimental data are indicated in Table 1, using the color coding of Matlab plots as listed in the table. For comparison we have repeated the data of maltopolymers (cyan symbols) and small sugars (magenta symbols). (For interpretation of the references to color in this figure legend, the reader is referred to the Web version of this article.)

temperatures. ( $\eta_{ref}$  is the zero shear viscosity at some arbitrary taken reference temperature  $T_{ref}$ ). The master curve for  $T_{ref} = 20^\circ\text{C}$  is shown in Fig. 5. A power law holds for high shear rates ( $\dot{\gamma}\tau_{ref}\eta_0/\eta_{ref} \gg 1$ ). Note,  $\tau_{ref} = 1/\dot{\gamma}_{cr,ref}$ , is an arbitrary shift factor, related to the critical shear rate  $\dot{\gamma}_{cr,ref}$  at reference conditions.

The scaling exponent is  $n = 0$ , as obtained via fitting. Shear thinning of maltodextrins is also observed by (Castro et al., 2016), who have measured maltodextrins with  $2 \leq DE \leq 19$ .

Furthermore, we have collected data sets from literature regarding extruded starch rheology, which are listed in Table 2. For most of these studies an extruder is used, but for the rice and oat flour extrusion is performed using a capillary rheometer. It is assumed that all starch crystallites have melted during extrusion, which happened before the rheological measurement. Starch might have degraded during extrusion (Della Valle et al., 1995), lowering the average molar weight and slightly modifying the  $T_g$  - as inferred by the Fox-Flory relation (Van der Sman &

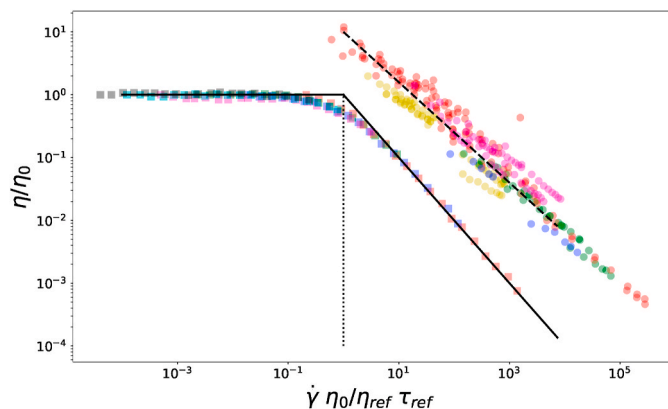


**Fig. 5.** Superposition of flow curves for MDX DE18 (circles) (Sillick & Gregson, 2009; Sillick & Gregson, 2009) and starch with data sources and color codes shown in Table 2. Horizontal and vertical shifting is performed with the zero-shear viscosity  $\eta_0$ . Shear-thinning exponent for MDX18 is  $n = 0$  (solid line), and for starch  $n = 0.2$  (dashed line), as obtained by fitting. (For interpretation of the references to color in this figure legend, the reader is referred to the Web version of this article.)

**Table 1**

Sources of literature data on viscosity of maltodextrins and sugars, with temperature ( $T$ ) and moisture content (M.C.) ranges, and the symbols used in the plots of Figs. 2–4.

Compound	$T_{g,s}$ (K)	Reference	$T(^{\circ}\text{C})$	M.C.	symbol
Fructose	306	(Migliori et al., 2007)	0–20	5–70%	m*
Fructose	306	(Rampp et al., 2000)	–15..20	30–85%	mv
Fructose	306	(Telis et al., 2007)	0..85	10–60%	mv
Glucose	306	(Migliori et al., 2007)	0..20	5–70%	m*
Glucose	306	(Telis et al., 2007)	0..85	10–60%	mv
Sucrose	336	(Migliori et al., 2007)	0..20	5–70%	m*
Sucrose	336	(Telis et al., 2007)	0..85	10–60%	mv
Maltose	353	(Noel et al., 1991)	0..100	75–90%	mo
Maltose	353	(Dupas-Langlet et al., 2019)	–20..80	71–99%	m+
MDX DE2	463	(Dupas-Langlet et al., 2019)	–20 .. 80	51–99%	c+
MDX DE18	388	(Normand et al., 2019)	55–90	68–91%	cs
MDX DE5	451	(Siemons et al., 2020)	20–80	20–77%	k.
MDX DE12	432	(Siemons et al., 2020)	20–80	20–77%	b.
MDX DE21	407	(Siemons et al., 2020)	20–80	20–77%	g.
MDX DE29	384	(Siemons et al., 2020)	20–80	20–77%	y.
MDX DE38	359	(Siemons et al., 2020)	20–80	20–77%	r.
MDX DE18/ sucrose 50:50	350	(Sillick & Gregson, 2009)	0..130	78–96%	c*
MDX DE2/MAL 20:80	360	(Dupas-Langlet et al., 2019)	–20 .. 80	51–99%	yo
MDX DE2/MAL 50:50	378	(Dupas-Langlet et al., 2019)	–20 .. 80	51–99%	r*
MDX DE2/MAL 80:20	418	(Dupas-Langlet et al., 2019)	–20 .. 80	51–99%	ks

**Table 2**

Data sources used for shear thinning master curve of starch.

System	Reference	Symbols
Normal Corn Starch	(Vergnes & Villemaire, 1987; Vergnes & Villemaire, 1987)	ro
	(Vergnes et al., 1993; Vergnes et al., 1993)	yo
	(Xie et al., 2009; Xie et al., 2009)	go
Waxy Corn Starch	(Xie et al., 2009; Xie et al., 2009)	bo
Rice Flour	(Dautant et al., 2007; Dautant et al., 2007)	mo

Meinders, 2011). But, we assume the average chain length is still high and comparable to that of a low DE maltodextrin ( $DE \approx 1$ ). Hence, we estimated  $\eta_0$  based on the zero-shear viscosity of the MDX DE2, as shown in Fig. 2.

It is striking that the starch data from this large collection of datasets fall on a single master curve, albeit with some variability in the data, which can be attributed to variations in molecular weight due to degradation or amylose content. The collected data is only in the shear-thinning regime, with an exponent different from the MDX18 - namely  $n = 0.2$ . Note that the rescaled data of starch exceeds the value  $\eta/\eta_0$ , meaning that the actual zero-shear viscosity of starch is higher than MDX DE2, or that the viscosity is diverging due to gelation of the starch via the amylose junctions, as observed for other polymer systems - showing critical gel behaviour (Li et al., 1997; Suman & Joshi, 2020; Winter 1987).

#### 4. Oscillatory rheology

We have collected experimental data of oscillatory rheology from literature on maltodextrin (Palzer, 2009; Kasapis & Shrinivas, 2010; Dupas-Langlet et al., 2019), and starch (Kasapis et al., 2000; Kristiawan et al., 2016). The collected data covers a wide range of temperatures and moisture contents. We analyze whether master curves can be constructed from the experimental data via time-temperature superposition principle. A convenient test of whether the latter principle holds is to explore to which extent they follow Cole-Cole plots or van Gurp-Palmen plots (Han & Kim, 1993; Van Gurp & Palmen, 1998; Trinkle & Friedrich, 2001). Here, one either plots  $\log(G')$  versus  $\log(G'')$ , or  $\log(G^*)$  versus  $\log(\tan(\delta)) = \log(G''/G')$ . The raw data from maltodextrin (Dupas-Langlet et al., 2019) and starch (Kristiawan et al., 2016) shows quite some scatter in the Cole-Cole plots and the van Gurp-Palmen plots. For example, the raw data is showing variation of the plateau value of  $G'_\infty$  in the glassy state. This variation of  $G'_\infty$  in the starch data is shown in figure B2, where it is shown to be a linear function of  $T/T_g$ , with  $T_g$  estimated via Couchman-Karasz cf. (Van der Sman & Meinders, 2011). The dataset of maltodextrin, maltose, and water is not showing such a correlation with  $T/T_g$ , which can be due to modulation of  $G'_\infty$  via antiplasticization effects imparted by the mixture of maltose and water (Townrow et al., 2010). The Cole-Cole and van Gurp-Palmen plots improve if the moduli are scaled against  $G'_\infty$ , as shown in figures B3-B.4. The maltodextrin data appear to approach the plateau zone, but with different  $G_N$  for different mixtures. However, for the regime of  $G' > 10$  MPa time-temperature superposition appears to be possible, as the data of starch and maltodextrin seem to follow a single curve, albeit still with a large variation.

For the superposition of the experimental data, we have used both the elastic modulus  $G'$  and the loss modulus  $G''$ , which is mapped onto the general master curve generated with the Marin-Graessley model. This mapping is via minimization of the least-squares of the distance between the Marin-Graessley master curve and the shifted experimental data. We think this superposition of curves with help of the Marin-Graessley model has advantages over the traditional (manual) procedures of spuer position, as it supposes some relation between  $G'$  and the loss modulus  $G''$  and certain shape of the curves. These constraints imposed by the model will increase the reliability and accuracy of the shift factors  $a_T$ .

Details of the used algorithm are described in the Appendix. Via an iterative process, we have determined the Marin-Graessley model parameters scaling exponent  $\alpha$ , the relaxation times  $\tau_M$  and  $\tau_\alpha$ , and the plateau values  $G_N$  and  $G_\infty$ . As reference value we have set  $\tau_\alpha = 0.5$  s. For all datasets analysed holds that there is no data available for the terminal zone. Hence,  $\tau_M$  could not be fitted, and it is set at an arbitrary (large) value of  $\tau_M = 1000$  s. Thus, the relevant fitting parameters are  $\alpha$ ,  $G_N$  and  $G_\infty$ .

The constructed master curves are shown in top panes of Figs. 6 and 7. Observe they are very similar to the expected master curves of transient networks, as shown in Fig. 1. The horizontal shift factors are shown in the bottom pane of figures Figs. 6 and 7. Despite some variability, one can conclude that the horizontal shift factor  $a_T$  is indeed a function of  $T_g/T$ , as expected from the transient network theory. For both starch and maltodextrin there is a discontinuity in the gradient of  $\log(a_T)$  versus  $T_g/T$  if  $T_g > T$ .

The exponent  $\alpha$  is different for starch and maltodextrin:  $\alpha = 0.215$  in the case of starch, and  $\alpha = 0.60$  in case of maltodextrin. If  $\alpha < 0.5$  the elastic modulus dominates over the loss modulus in the transient regime - which holds for starch. For maltodextrin  $\alpha > 0.5$  where the loss modulus is larger than the elastic modulus for a finite frequency window in the transient regime. This is in agreement with the observation by (Dupas-Langlet et al., 2019), where it is stated that in this regime the phase angle indeed exceeds  $45^\circ$ . For starch, it is observed that the phase angle never exceeds  $45^\circ$  (Kristiawan et al., 2016). If the Cox-Merz rule holds, the exponent  $\alpha$  is expected to be identical to the shear-thinning

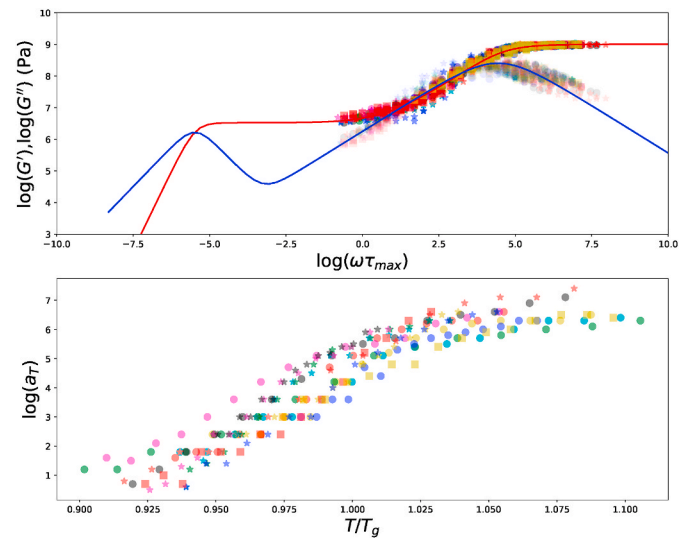


**Fig. 6.** Master curve of maltodextrin DE2 fitted to Marin-Graessley model with data from (Dupas-Langlet et al., 2019). Fitted model parameters is  $\alpha = 0.60$ ,  $G_\infty = 1$  GPa,  $G_N = 3$  MPa,  $\tau_M = 1000$  s, and  $\tau_\alpha = 0.5$  s. Both horizontal and vertical shifting is applied. Horizontal shift factor  $a_T$  appears to scale with  $T_g/T$ .

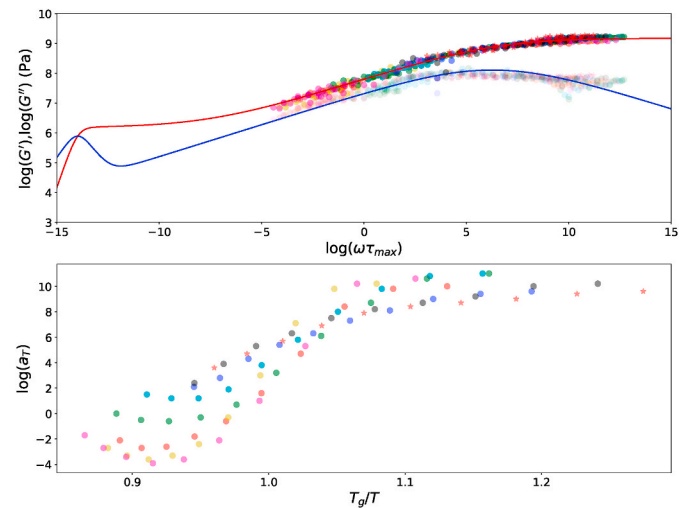


**Fig. 7.** Master curve of starch fitted to Marin-Graessley model with data from (Kristiawan et al., 2016). Fitted model parameters is  $\alpha = 0.215$ ,  $G_\infty = 1.5$  GPa,  $G_N = 1.5$  MPa,  $\tau_M = 1000$  s, and  $\tau_\alpha = 0.5$  s. Only horizontal shifting is applied. Horizontal shift factor  $a_T$  appears to scale with  $T_g/T$ .

exponent  $n$ . For starch, we have found  $\alpha = 0.215$ , which is well in agreement with the shear thinning exponent  $n = 0.2$  as shown in Fig. 5.

It is satisfying that all mixtures of maltopolymer, maltose, and water can be mapped to a single master curve, whereby we note that there is still some variation between the various samples compositions apparent. Even the maltose/water mixture falls on the constructed master curve. We conclude that maltose only modulates the  $T_g$  of the ternary mixture. The mixture of water and maltose can be viewed as effectively a single solvent/plasticizer. Similarly, for the rheology of resilin (Khandaker et al., 2017) and gluten (Costanzo et al., 2020) a similar “single solvent” effect is found for ethanol/water mixtures. Here ethanol can be viewed as a plasticizer/solvent (Yu & Baird, 2019). Furthermore, we have observed related behaviour for mixtures of plasticizers influencing the melting transitions of biopolymers (van der Sman, 2016). There we have stated that the mixture of plasticizers is characterized by the hydrogen bond density,  $n_{OH,eff}$ , which is shown to be correlated to the viscosity  $\eta$  and thus  $T_g/T$  (van der Sman & Mauer, 2019).

We have also investigated other datasets from literature, namely a) gelatinized wheat starch (Kasapis et al., 2000), and maltodextrin DE42 (Kasapis & Shrinivas, 2010), with results shown in Fig. 8. The starch data is now showing response in the plateau zone, which has to be modelled with the three-mode Marin-Graessley model. The starch data is not fitting optimally in the transition zone and the first part of the plateau zone. The maltodextrin data is showing response of the transition zone and glassy zone only. The magnitude of  $G_\infty$  is quite large, compared to the other data sets.

The general trend in the data is that the horizontal shift factor is a function of  $T_g/T$ . The magnitude of  $G_\infty$  is in the range  $0.1 < G_\infty < 10$  GPa, but quite dependent on a particular dataset. The width of the transient regime, indicated by  $\tau_M$  and  $\tau_\alpha$ , is very similar for all datasets. The relation of the horizontal shift factor  $\log(a_T)$  with  $T_g/T$  is showing a discontinuity in the gradient at  $T_g/T = 1$ . The change of  $a_T$  with temperature is significantly smaller in the glassy regime, if  $T_g/T > 1$ . A change in the temperature dependency of the horizontal shift factor at  $T = T_g$  has been observed earlier (Kasapis et al., 2000).

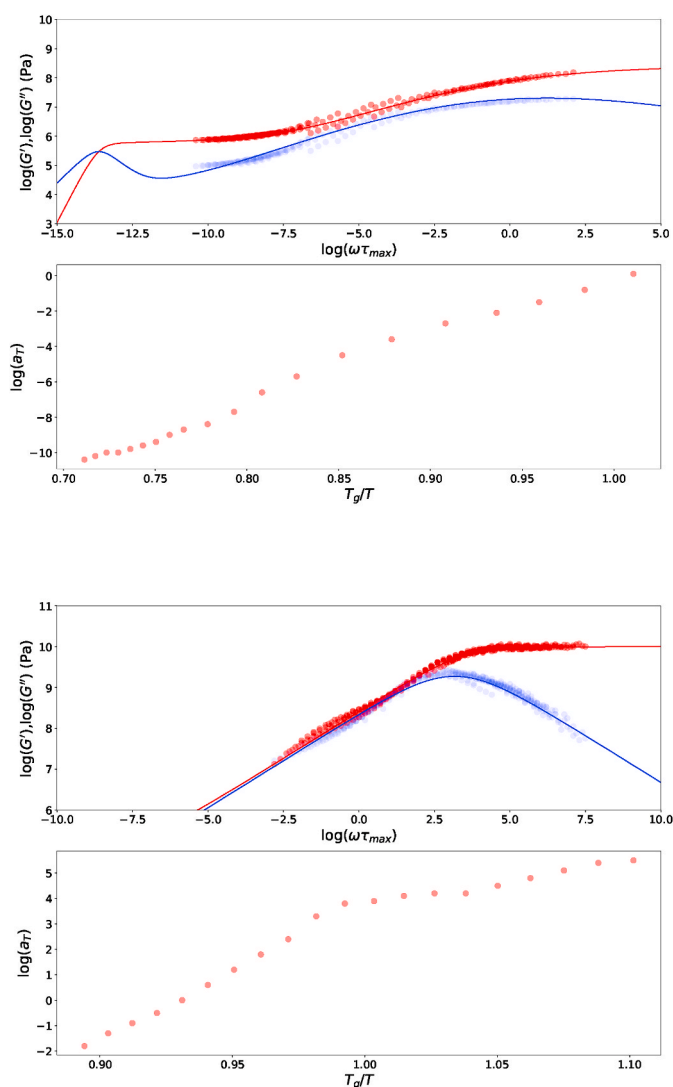


**Fig. 8.** a) Master curve of wheat starch fitted to 3-mode Marin-Graessley model with data from (Kasapis et al., 2000). Fitted model parameters are  $\alpha = 0.36$ ,  $p = 0.18$ ,  $G_\infty = 0.25$  GPa,  $G_N = 1$  MPa,  $\tau_M = \tau_p = 10^3$  s,  $\tau_\alpha = 0.5$  s,  $k_p = 165$ , and  $k_\alpha = 300$ . Only horizontal shifting is applied. Horizontal shift factor  $a_T$  appears to scale with  $T_g/T$ . b) Master curve of MDX DE42 fitted to 2-mode Marin-Graessley model with data from (Kasapis & Shrinivas, 2010). Fitted model parameters are  $\alpha = 0.46$ ,  $G_\infty = 10$  GPa,  $\tau_M = 10^3$  s,  $\tau_\alpha = 0.5$  s,  $k_\alpha = 10^5$ . Only horizontal shifting is applied. Horizontal shift factor  $a_T$  is a function of  $T_g/T$ .

## 5. Discussion

From the above analysis follows that in the many aspects of the rheology of starch and maltodextrins the ratio  $T_g/T$  is the dominant governing parameter. The zero-shear viscosity is a function of  $T_g/T$ , and relates to the horizontal and vertical shift factors used to construct master curves of the shear-dependent viscosities. Furthermore,  $T_g/T$  is related to the horizontal shift factors applied in the construction of master curves from the SAOS data. In this section, we discuss our findings in view of existing literature.

We start the discussion with the comparison of our analysis with a recent study using the same dataset on zero-shear viscosity of maltopolymer/maltose mixtures (Ubbink & Dupas-Langlet, 2020). Here, the data has been analysed using a modified WLF-theory. Commonly, WLF theory is applied using the universal constants  $C_1$ , and  $C_2$ . In the modified WLF theory the  $C_1$  and  $C_2$  are considered free parameters, and moreover,  $C_2$  is considered to be a function of the water content, with 3 additional free parameters. The experimental data have been fitted to the modified WLF theory, but the set of four fitted parameters has been estimated separately for each dataset. While some trends in the fitted values of the parameters could be observed, at this stage the model does not allow to discriminate between various physical models that may underlie the different maltopolymer/maltose mixtures.

We like to remark, that our analysis above did not involve any fitting of theory to the viscosity data, except for fitting the modified Couchman-Karasz to the glass transition data. Of the same maltopolymer/maltose mixtures also SAOS data was available, which we have analysed above. The analysis of the SAOS data much more clearly shows that their rheology is governed by the ratio of  $T_g/T$ . Hence, we expect that this also holds for the zero-shear viscosity. Whether it holds for the maltopolymer/maltose mixtures that the zero-shear viscosity falls into two distinct classes requires further investigation. But, our analysis of zero-shear viscosity on polydisperse maltodextrins (Siemons et al., 2020) seems to confirm our hypothesis of the two distinct classes. In a forthcoming paper, analysing the effects of dextrose equivalence (DE) on rheology (Siemons et al., 2021), the same classification of polydisperse maltodextrins is found concerning their rheological behaviour. The results of this paper is summarized in the [Supplementary Material \(Figs. B5-B.12\)](#). As one can observe there, DE5 and DE12 are showing a master curve with a distinct plateau zone, as shown for DE2 in this paper. The scaling exponent of the transition zone is  $\alpha = 0.65$  and  $\alpha = 0.6$  for DE5 and DE12 respectively, which is in good agreement with the value for DE2, as determined in this study. However, the plateau modulus  $G_N$  decreases with increasing DE value. The master curves for DE21, DE38, and DE42 are lacking this plateau zone, but only exhibit a transition and glassy zone. The scaling exponent in the transition zone is about  $\alpha = 1.0$ , which is a consequence of their behaviour as a Newtonian viscous liquid.

This lack of a plateau zone is explained by the fact that these short oligosaccharides can not entangle. In literature, it is claimed that for entanglements of maltodextrins a minimal degree of polymerization ( $DP \sim 1/DE$ ) is required (Levine & Slade, 1986). states that it requires  $DE \leq 6$  for entanglement, while (Castro et al., 2016) states that entanglement is observed for  $DE \leq 12$ , and that plastic behaviour is observed for DE17 and DE19. This is largely in agreement with the entanglement threshold of  $DE < 18$  by (Biliaderis et al., 1999). There, it is also stated that entanglement also depends on the precise molecular weight distribution. Interaction between different chains is described in (Kutzi et al., 2019), where it is stated that the polymer chains of DE 12 and 21 were too short to contribute to the entangled network of the long DE 2 chains, but they were long enough to interfere with their entanglement. Hence, the division of maltodextrins in two classes concerning their zero-shear viscosity is thus very likely explained by their capability to entangle. We think it will be valuable to extend the investigation of the two distinct scaling regimes for zero shear viscosity to other (concentrated) biopolymers.



Shear-thinning behaviour is linked to an entangled polymer network that is disturbed at sufficiently high shear rates (Kriegel et al., 2009). In Fig. 5 we have shown shear-thinning behaviour for starch (with  $DE < 1$ ) and for maltodextrin with  $DE = 18$ . This observation is in agreement with the above threshold for entanglement, which is  $DE_{cr} \approx 18$ . Shear-thinning behaviour of maltodextrins is observed up to  $DE \leq 19$ , but from differences in the shear-thinning exponents it is concluded that maltodextrins with  $17 \leq DE \leq 19$  have a very low degree of entanglement.

As suggested by one of our reviewers, we compare the different relations of  $a_T$  versus  $T_g/T$  for the different maltodextrins in a single graph, which is shown in Fig. 9. Because for the different maltodextrins we have used different reference temperatures for  $a_T$  we have performed vertical shifting of  $a_T$  such that  $a_T(T = T_g) \approx 1$ . Furthermore, we have allowed for a small horizontal shift of maximal 5%, to maximize superposition. It is expected that the horizontal shift factors for the oscillatory rheology coincide with that of the zero-shear viscosity:  $a_T = \eta_0/\eta_g$ , with  $\eta_g$  the viscosity at the glass transition (Ubbink & Dupas-Langlet, 2020). Hence, in Fig. 9 we have also drawn the relation  $\eta_0/\eta_g$  versus  $T_g/T$ . Despite the variability in the experimental data, one can observe from Fig. 9 that all shift factors largely follow the expected trend, as indicated by the zero-shear viscosity. This is especially in the range  $0.9 < T_g/T < 1$  where the response is dominated by the  $\alpha$ -relaxation. For  $T_g/T > 1$  the shift factors  $a_T$  are leveling off, while the zero-shear viscosity appears to show divergent behaviour in this regime. One might conclude there is an apparent breakdown of the superposition principle. Yet, zero-shear is viscosity can not be measured directly. We leave this point for further research. For the conditions that are relevant for processing  $T_g/T < 1$  there is sufficient ground for assuming simple rheological behaviour, which allows for consistent superposition in zero-shear viscosity, flow curves and oscillatory rheology.

We have also included the starch data in this plot (data not shown). The starch data shows overlap in the range  $0.9 < T_g/T < 1.0$ , but shows deviations in the range  $T_g/T < 0.9$  - which is why the starch data set is not included. Hence, while there is similarity in the  $\alpha$ -relaxations, deviations occur when the starch is away from the glass transition. Extruded starch can have different amounts of retrogradation of amylose, acting as crosslinkers, giving rise to different plateau-moduli. Observing individual datasets from (Kristiawan et al., 2016) indeed shows the onsets of a plateau-zone, but at different levels of  $G_N$ . Maltodextrins do show a consistent level of  $G_N$ , as one can observe in the

**Supplementary Material.** We expect that (extruded) starch will not be simple rheological material, due to the crystallizing (retrogradation) tendency of amylose and amylopectin. Of course, native (ungelatinized) starches are present as starch granules suspended in water, which is expected to give totally different rheological behaviour than (extruded) ungelatinized starch.

Liu has proposed a slightly modified scaling relation (Liu et al., 2006):

$$\log(a_T) \sim \frac{T_g}{T - 0.77T_g} = \frac{1}{T/T_g - 0.77} \quad (10)$$

While in a related study (Siemons et al., 2021) we have confirmed this scaling for polydisperse maltodextrins in the range  $0.5 < T_g/T < 1$ , we view that this scaling does not comply with our found scaling of the shift factor in the range  $T_g/T > 1$ . According to the scaling relation of Liu, the shift factor should diverge at  $T_g/T = 1/0.77 = 1.3$ . However, we have found that  $\log(a_T)$  levels off in the regime  $T_g/T > 1$  instead of diverging. Such levelling off is in compliance with our studies in literature (Kasapis et al., 2000). Other studies also found scaling of rheological parameters with  $T_g/T$  as the zero shear viscosity of honeys (Andraca et al., 2013), but found a linear scaling of  $\log(a_T)$  with  $(T_g/T)^2$  in the range  $0.5 < (T_g/T)^2 < 0.8$ . Structural relaxation in sucrose/glycerol is shown to scale with  $T_g/T$ , with a leveling off in the range of  $T_g/T > 1$  (You & Ludescher, 2007). For polydisperse polyamides differing in molecular weight it is found that horizontal shift factors scale with  $T_g/T$  (de Figueiredo Martins, 2019), albeit it was a non-linear relation in the range  $0.85 < T_g/T < 1$ . Deviation from the “universal” relation is found if ionic groups are present in the polyamide.

The found scaling of horizontal shift factors  $a_T$  with  $T_g/T$  is also in line with various studies on time-temperature-moisture superposition (Fabre et al., 2018; Ishisaka et al., 2004; Krauklis et al., 2019; Patankar et al., 2008; Zhan et al., 2019; Zhang et al., 2020). This superposition is found for materials, where hydrogen bonding is important, such as wood, polyelectrolytes, polyamides, and epoxies. Only, one paper in this field has made a connection of the shift factors to  $T/T_g$  (Krauklis et al., 2019).

Given the similarity between polyamides and proteins (Bradbury & Elliott, 1963), the similar findings for maltodextrins and polyamides, as discussed above, we assume that the theory of transient networks would also apply to proteins, having a random coil-like configuration, like gluten, gelatin, elastin, casein, silk and resilin. Some observations on protein rheology (Popineau et al., 1994; Redl, Morel, Bonicel, Guilbert, & Vergnes, 1999,a; Larré et al., 2000; Pruska-Kedzior et al., 2008; Khandaker et al., 2017; Costanzo et al., 2020) as already mentioned in the introduction, give credit to this assumption.

## 6. Conclusions

In this paper, it is shown that much of the rheological behaviour of concentrated polysaccharides is governed by the ratio  $T_g/T$ . First, we have shown this scaling for the zero shear viscosity of long maltodextrins, which has shown a similar scaling relation as small carbohydrates, albeit it was one magnitude larger. Using time-temperature superposition based on the zero shear viscosity, we showed that the Carreau-Yasuda model well describes the flow curves. Based on the zero shear viscosity maltodextrins can be divided into two distinct classes, each showing a different scaling with  $T_g/T$ , which can be attributed to the occurrence of entanglement. The maltodextrins showing entanglement also exhibits shear-thinning behaviour. The critical DE value for entanglement is approximately  $DE_{cr} = 18$ .

Ultimately, we have shown that the  $T_g/T$  scaling holds for small-amplitude oscillatory rheology of maltodextrins and starches, all showing a master curve following the Marin-Graessley model. The horizontal shift factor  $a_T$  for constructing the master curve is shown to be a function of  $T_g/T$ . Remarkably, the relation between  $\log(a_T)$  and  $T_g/T$  is

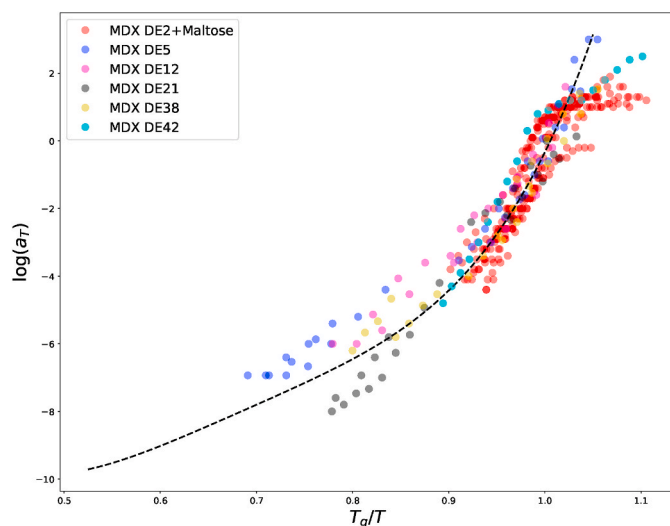


**Fig. 9.** Comparison of the shift factors  $a_T$  versus  $T_g/T$  for the various maltodextrins investigated, after application of vertical shifting such that  $a_T(T = T_g) \approx 1$ . The dashed line indicates the expected shift factors following the fitted zero-shear viscosity relation, as shown in Fig. 2.

showing a discontinuity of its gradient at  $T_g/T = 1$ . The constructed SAOS master curve is showing that the investigated polysaccharides are showing three different zones: a plateau zone, a transient zone, and a glassy zone, similar to master curves known in literature for synthetic linear polymers, behaving as transient entangled networks.

## Author statement

RGM van der Sman: Conceptualization; Methodology; Writing - original draft; review & editing.

Job Ubbink: Writing - review & editing.

Marina Dupas-Langlet: Data curation; Investigation; Writing - review.

Magdalena Kristiawan: Data curation; Investigation; Writing - review.

Isabel Siemons: Data curation; Investigation; Methodology; Writing - review.

## Declaration of competing interest

We declare there are no conflicts of interest.

## Appendix A. Supplementary data

Supplementary data to this article can be found online at <https://doi.org/10.1016/j.foodhyd.2021.107306>.

## References

- Agapov, A., Novikov, V., Hong, T., Fan, F., & Sokolov, A. (2018). Surprising temperature scaling of viscoelastic properties in polymers. *Macromolecules*, 51, 4874–4881.
- Aho, J., Boetker, J., Baldursdottir, S., & Rantanen, J. (2015). Rheology as a tool for evaluation of melt processability of innovative dosage forms. *International Journal of Pharmaceutics*, 494, 623–642.
- Aho, J., & Syrjäälä, S. (2008). On the measurement and modeling of viscosity of polymers at low temperatures. *Polymer Testing*, 27, 35–40.
- Andraca, A., Goldstein, P., & del Castillo, L. (2013). Description of the viscosity of honeys in the supercooled regime. *Physica A: Statistical Mechanics and Its Applications*, 392, 6206–6213.
- Angell, C. (2002). Liquid fragility and the glass transition in water and aqueous solutions. *Chemical Reviews*, 102, 2627–2650.
- Ashokan, B. K., & Kokini, J. L. (2005). Determination of the wlf constants of cooked soy flour and their dependence on the extent of cooking. *Rheologica Acta*, 45, 192–201.
- Avaltroni, F., Bouquerand, P., & Normand, V. (2004). Maltodextrin molecular weight distribution influence on the glass transition temperature and the melt flow behavior for gluten, casein and soya. *Journal of Cereal Science*, 45, 275–284.
- Biliaderis, C., Swan, R., & Arvanitoyannis, I. (1999). Physicochemical properties of commercial starch hydrolyzates in the frozen state. *Food Chemistry*, 64, 537–546.
- Both, E., Siemons, I., Boom, R., & Schutyser, M. (2019). The role of viscosity in morphology development during single droplet drying. *Food Hydrocolloids*, 94, 510–518.
- Bradbury, E., & Elliott, A. (1963). Infra-red spectra and chain arrangement in some polyamides, polypeptides and fibrous proteins. *Polymer*, 4, 47–59.
- Caputo, M., Selb, J., & Candau, F. (2004). Effect of temperature on the viscoelastic behaviour of entangled solutions of multisticker associating polyacrylamides. *Polymer*, 45, 231–240.
- Castro, N., Durrieu, V., Raynaud, C., & Rouilly, A. (2016). Influence of de-value on the physicochemical properties of maltodextrin for melt extrusion processes. *Carbohydrate Polymers*, 144, 464–473.
- Cervone, N., & Harper, J. (1978). Viscosity of an intermediate moisture dough. *Journal of Food Process Engineering*, 2, 83–95.
- Costanzo, S., Banc, A., Louhichi, A., Chauveau, E., Wu, B., Morel, M., & Ramos, L. (2020). Tailoring the viscoelasticity of polymer gels of gluten proteins through solvent quality. *Macromolecules*, 53, 9470–9479.
- Dautant, F., Simancas, K., Sandoval, A., & Müller, A. (2007). Effect of temperature, moisture and lipid content on the rheological properties of rice flour. *Journal of Food Engineering*, 78, 1159–1166.
- Della Valle, G., Boche, Y., Colonna, P., & Vergnes, B. (1995). The extrusion behaviour of potato starch. *Carbohydrate Polymers*, 28, 255–264.
- Della Valle, G., Colonna, P., Patria, A., & Vergnes, B. (1996). Influence of amylose content on the viscous behavior of low hydrated molten starches. *Journal of Rheology*, 40, 347–362.
- Descamps, N., Palzer, S., Roos, Y., & Fitzpatrick, J. (2013). Glass transition and flowability/caking behaviour of maltodextrin de 21. *Journal of Food Engineering*, 119, 809–813.
- D'Haene, P., & Van Liederkerke, B. (1996). Viscosity prediction of starch hydrolysates from single point measurements. *Starch-Stärke*, 48, 327–334.
- Ding, Y., & Sokolov, A. P. (2006). Breakdown of time-temperature superposition principle and universality of chain dynamics in polymers. *Macromolecules*, 39, 3322–3326.
- Dupas-Langlet, M., Meunier, V., Pouzot, M., & Ubbink, J. (2019). Influence of blend ratio and water content on the rheology and fragility of maltopolymer/maltose blends. *Carbohydrate Polymers*, 213, 147–158.
- Fabre, V., Quandalle, G., Billon, N., & Cantournet, S. (2018). Time-temperature-water content equivalence on dynamic mechanical response of polyamide 6, 6. *Polymer*, 137, 22–29.
- Fatкуллин, N., Mattea, C., & Stapf, S. (2011). A simple scaling derivation of the shear thinning power-law exponent in entangled polymer melts. *Polymer*, 52, 3522–3525.
- de Figueiredo Martins, A. (2019). *Effect of intermolecular interactions on the viscoelastic behavior of polyamides*. Ph.D. thesis. Université de Lyon.
- Gholamipour-Shirazi, A., Norton, I., & Mills, T. (2019). Designing hydrocolloid based food-ink formulations for extrusion 3d printing. *Food Hydrocolloids*, 95, 161–167.
- Gianfrancesco, A., Turchiuli, C., Flick, D., & Dumoulin, E. (2010). Cfd modeling and simulation of maltodextrin solutions spray drying to control stickiness. *Food and Bioprocess Technology*, 3, 946–955.
- Groot, R., & Agerof, W. (1995). Dynamic viscoelastic modulus of associative polymer networks: Off-lattice simulations, theory and comparison to experiments. *Macromolecules*, 28, 6284–6295.
- Han, C., & Kim, J. (1993). On the use of time-temperature superposition in multicomponent/multiphase polymer systems. *Polymer*, 34, 2533–2539.
- Heo, Y., & Larson, R. (2005). The scaling of zero-shear viscosities of semidilute polymer solutions with concentration. *Journal of Rheology*, 49, 1117–1128, 1978-present.
- Hughes, D., Bönisch, G., Zwick, T., Schäfer, C., Tedeschi, C., Leuenberger, B., Martini, F., Mencarini, G., Geppi, M., Alam, M., & Ubbink, J. (2018). Phase separation in amorphous hydrophobically modified starch-sucrose blends: Glass transition, matrix dynamics and phase behavior. *Carbohydrate Polymers*, 199, 1–10.
- Imamura, K., Fukushima, A., Sakaura, K., Sugita, T., Sakiyama, T., & Nakanishi, K. (2002). Water sorption and glass transition behaviors of freeze-dried sucrose-dextran mixtures. *Journal of Pharmaceutical Sciences*, 91, 2175–2181.
- Ishisaka, A., & Kawagoe, M. (2004). Examination of the time-water content superposition on the dynamic viscoelasticity of moistened polyamide 6 and epoxy. *Journal of Applied Polymer Science*, 93, 560–567.
- Jensen, M., Gainaru, C., Alba-Simionesco, C., Hecksher, T., & Niss, K. (2018). Slow rheological mode in glycerol and glycerol-water mixtures. *Physical Chemistry Chemical Physics*, 20, 1716–1723.
- Kasapis, S., Sablani, S., & Biliaderis, C. (2000). Dynamic oscillation measurements of starch networks at temperatures above 100 °C. *Carbohydrate Research*, 329, 179–187.
- Kasapis, S., & Shrinivas, P. (2010). Combined use of thermomechanics and uv spectroscopy to rationalize the kinetics of bioactive compound (caffeine) mobility in a high solids matrix. *Journal of Agricultural and Food Chemistry*, 58, 3825–3832.
- Khandaker, M., Dudek, D., Beers, E., & Dillard, D. (2017). Expression, crosslinking, and developing modulus master curves of recombinant resilin. *Journal of the Mechanical Behavior of Biomedical Materials*, 69, 385–394.
- Kilburn, D., Claude, J., Schweizer, T., Alam, A., & Ubbink, J. (2005). Carbohydrate polymers in amorphous states: An integrated thermodynamic and nanostructural investigation. *Biomacromolecules*, 6, 864–879.
- Krauklis, A., Akulichev, A., Gagani, A., & Echtermeyer, A. (2019). Time-temperature-plasticization superposition principle: Predicting creep of a plasticized epoxy. *Polymers*, 11, 1848.
- Kriegel, C., Kit, K., McClements, D., & Weiss, J. (2009). Electrospinning of chitosan-poly (ethylene oxide) blend nanofibers in the presence of micellar surfactant solutions. *Polymer*, 50, 189–200.
- Kristiawan, M., Chaunier, L., Della Valle, G., Lourdin, D., & Guessasma, S. (2016). Linear viscoelastic properties of extruded amorphous potato starch as a function of temperature and moisture content. *Rheologica Acta*, 1–15.
- Kristiawan, M., Della Valle, G., Kansou, K., Ndiaye, A., & Vergnes, B. (2019). Validation and use for product optimization of a phenomenological model of starch foods expansion by extrusion. *Journal of Food Engineering*, 246, 160–178.
- Kutzli, I., Beljo, D., Gibis, M., Baier, S., & Weiss, J. (2019). Effect of maltodextrin dextrose equivalent on electrospinnability and glycation reaction of blends with pea protein isolate. *Food Biophysics*, 1–10.
- Lai, L., & Kokini, J. (1991). Physicochemical changes and rheological properties of starch during extrusion. (A review). *Biotechnology Progress*, 7, 251–266.
- Larré, C., Denery-Papini, S., Popineau, Y., Deshayes, G., Desserme, C., & Lefebvre, J. (2000). Biochemical analysis and rheological properties of gluten modified by transglutaminase. *Cereal Chemistry*, 77, 121–127.
- Levine, H., & Slade, L. (1986). A polymer physico-chemical approach to the study of commercial starch hydrolysis products (shps). *Carbohydrate Polymers*, 6, 213–244.
- Liu, Z., Bhandari, B., Prakash, S., Mantihal, S., & Zhang, M. (2019). Linking rheology and printability of a multicomponent gel system of carrageenan-xanthan-starch in extrusion based additive manufacturing. *Food Hydrocolloids*, 87, 413–424.
- Li, L., Uchida, H., Aoki, Y., & Yao, M. (1997). Rheological images of poly (vinyl chloride) gels. 2. Divergence of viscosity and the scaling law before the sol-gel transition. *Macromolecules*, 30, 7842–7848.
- Liu, C., He, J., Keunings, R., & Bailly, C. (2006). New linearized relation for the universal viscosity-temperature behavior of polymer melts. *Macromolecules*, 39, 8867–8869.
- Maranas, J. K. (2007). The effect of environment on local dynamics of macromolecules. *Current Opinion in Colloid & Interface Science*, 12, 29–42.

- Marin, G., & Graessley, W. (1977). Viscoelastic properties of high molecular weight polymers in the molten state. *Rheologica Acta*, 16, 527–533.
- Martini, F., Hughes, D., Bönisch, G., Zwick, T., Schäfer, C., Geppi, M., Alam, M., & Ubbink, J. (2020). Antiplasticization and phase behavior in phase-separated modified starch-sucrose blends: A positron lifetime and solid-state nmr study. *Carbohydrate Polymers*, 250, 116931.
- Masavang, S., Roudaut, G., & Champion, D. (2019). Identification of complex glass transition phenomena by dsc in expanded cereal-based food extrudates: Impact of plasticization by water and sucrose. *Journal of Food Engineering*, 245, 43–52.
- Mighri, F., Huneault, M., Ajji, A., Ko, G., & Watanabe, F. (2001). Rheology of epr/pp blends. *Journal of Applied Polymer Science*, 82, 2113–2127.
- Migliori, M., Gabriele, D., Di Sanzo, R., de Cindio, B., & Correr, S. (2007). Viscosity of multicomponent solutions of simple and complex sugars in water. *Journal of Chemical & Engineering Data*, 52, 1347–1353.
- Morris, E., Cutler, A., Ross-Murphy, S., Rees, D., & Price, J. (1981). Concentration and shear rate dependence of viscosity in random coil polysaccharide solutions. *Carbohydrate Polymers*, 1, 5–21.
- Noel, T., Ring, S., & Whittam, M. (1991). Kinetic aspects of the glass-transition behaviour of maltose—water mixtures. *Carbohydrate Research*, 212, 109–117.
- Normand, V., Armanet, L., McIver, R., & Bouquerand, P. (2019). Water diffusion in the semi-liquid state during industrial candy preparation. *Food Biophysics*, 14, 193–204.
- Palzer, S. (2009). Influence of material properties on the agglomeration of water-soluble amorphous particles. *Powder Technology*, 189, 318–326.
- Palzer, S. (2010). The relation between material properties and supra-molecular structure of water-soluble food solids. *Trends in Food Science & Technology*, 21, 12–25.
- Paradkar, A., Kelly, A., Coates, P., & York, P. (2009). Shear and extensional rheology of hydroxypropyl cellulose melt using capillary rheometry. *Journal of Pharmaceutical and Biomedical Analysis*, 49, 304–310.
- Patankar, K., Dillard, D., Case, S., Ellis, M., Lai, Y., Budinski, M., & Gittleman, C. (2008). Hygrothermal characterization of the viscoelastic properties of gore-select® 57 proton exchange membrane. *Mechanics of Time-dependent Materials*, 12, 221–236.
- Philipp, C., Emin, M., Buckow, R., Silcock, P., & Oey, I. (2018). Pea protein-fortified extruded snacks: Linking melt viscosity and glass transition temperature with expansion behaviour. *Journal of Food Engineering*, 217, 93–100.
- Popineau, Y., Cornec, M., Lefebvre, J., & Marchylo, B. (1994). Influence of high mr glutenin subunits on glutenin polymers and rheological properties of glutes and gluten subfractions of near-isogenic lines of wheat sicco. *Journal of Cereal Science*, 19, 231–241.
- Pruska-Kedzior, A., Kedzior, Z., & Klockiewicz-Kaminska, E. (2008). Comparison of viscoelastic properties of gluten from spelt and common wheat. *European Food Research and Technology*, 227, 199–207.
- Ramp, M., Buttersack, C., & Lüdemann, H. (2000). c, t-dependence of the viscosity and the self-diffusion coefficients in some aqueous carbohydrate solutions. *Carbohydrate Research*, 328, 561–572.
- Redl, A., Morel, M. H., Bonicel, J., Guilbert, S., & Vergnes, B. (1999). Rheological properties of gluten plasticized with glycerol: Dependence on temperature, glycerol content and mixing conditions. *Rheologica Acta*, 38, 311–320.
- Redl, A., Morel, M., Bonicel, J., Vergnes, B., & Guilbert, S. (1999a). Extrusion of wheat gluten plasticized with glycerol: Influence of process conditions on flow behavior, rheological properties, and molecular size distribution. *Cereal Chemistry*, 76, 361–370.
- Roudaut, G., & Wallecan, J. (2015). New insights on the thermal analysis of low moisture composite foods. *Carbohydrate Polymers*, 115, 10–15.
- Shamblin, S. L., Huang, E. Y., & Zografi, G. (1996). The effects of co-lyophilized polymeric additives on the glass transition temperature and crystallization of amorphous sucrose. *Journal of Thermal Analysis*, 47, 1567–1579.
- Shamblin, S. L., & Zografi, G. (1998). Enthalpy relaxation in binary amorphous mixtures containing sucrose. *Pharmaceutical Research*, 15, 1828–1834.
- Siemons, I., Polietiek, R., Boom, R., van der Sman, R., & Schutyser, M. (2020). Dextrose equivalence of maltodextrins determines particle morphology development during single sessile droplet drying. *Food Research International*, 131, 108988.
- Siemons, I., Vesper, J., Boom, R., Schutyser, M., & van der Sman, R. (2021). Rheological behaviour of concentrated maltodextrins describes skin formation and morphology development during droplet drying. *Food Hydrocolloids*. submitted for publication.
- Sillick, M., & Gregson, C. (2009). Viscous fragility of concentrated maltopolymer/sucrose mixtures. *Carbohydrate Polymers*, 78, 879–887.
- van der Sman, R. (2013). Predictions of glass transition temperature for hydrogen bonding biomaterials. *The Journal of Physical Chemistry B*, 117, 16303–16313.
- van der Sman, R. (2016). Sugar and polyol solutions as effective solvent for biopolymers. *Food Hydrocolloids*, 56, 144–149.
- van der Sman, R., & Broeze, J. (2014). Multiscale analysis of structure development in expanded starch snacks. *Journal of Physics: Condensed Matter*, 26, 464103.
- van der Sman, R., & Meinders, M. (2013). Moisture diffusivity in food materials. *Food Chemistry*, 138, 1265–1274.
- Sokolov, A., & Schweizer, K. (2009). Resolving the mystery of the chain friction mechanism in polymer liquids. *Physical Review Letters*, 102, 248301.
- Song, Y., Zheng, Q., & Wang, Z. (2007). Equibiaxial extensional flow of wheat gluten plasticized with glycerol. *Food Hydrocolloids*, 21, 1290–1295.
- Sritham, E., & Gunasekaran, S. (2017). Rheological and microstructure evaluations of amorphous sucrose-maltodextrin-sodium citrate mixture. *Applied Rheology*, 27, 1–10.
- Stadler, F., & Mahmoudi, T. (2011). Understanding the effect of short-chain branches by analyzing viscosity functions of linear and short-chain branched polyethylenes. *Korea-Australia Rheology Journal*, 23, 185–193.
- Suman, K., & Joshi, Y. (2020). On the universality of the scaling relations during sol-gel transition. *Journal of Rheology*, 64, 863–877.
- Taylor, L. S., & Zografi, G. (1998). Sugar-polymer hydrogen bond interactions in lyophilized amorphous mixtures. *Journal of Pharmaceutical Sciences*, 87, 1615–1621.
- Telis, V., Telis-Romero, J., Mazzotti, H., & Gabas, A. (2007). Viscosity of aqueous carbohydrate solutions at different temperatures and concentrations. *International Journal of Food Properties*, 10, 185–195.
- Townrow, S., Kilburn, D., Alam, A., & Ubbink, J. (2007). Molecular packing in amorphous carbohydrate matrixes. *The Journal of Physical Chemistry B*, 111, 12643–12648.
- Townrow, S., Roussanova, M., Giardiello, M., Alam, A., & Ubbink, J. (2010). Specific volume-hole volume correlations in amorphous carbohydrates: Effect of temperature, molecular weight, and water content. *The Journal of Physical Chemistry B*, 114, 1568–1578.
- Trinkle, S., & Friedrich, C. (2001). Van gorp-palmen-plot: A way to characterize polydispersity of linear polymers. *Rheologica Acta*, 40, 322–328.
- Ubbink, J. (2016). Structural and thermodynamic aspects of plasticization and antiplasticization in glassy encapsulation and biostabilization matrices. *Advanced Drug Delivery Reviews*, 100, 10–26.
- Ubbink, J., & Dupas-Langlet, M. (2020). Rheology of carbohydrate blends close to the glass transition: Temperature and water content dependence of the viscosity in relation to fragility and strength. *Food Research International*, 138, 109801.
- Ubbink, J., Giardiello, M., & Limbach, H. (2007). Sorption of water by bidisperse mixtures of carbohydrates in glassy and rubbery states. *Biomacromolecules*, 8, 2862–2873.
- Valle, G. D., Vergnes, B., & Lourdin, D. (2007). Viscous properties of thermoplastic starches from different botanical origin. *International Polymer Processing*, 22, 471–479.
- Van Gorp, M., & Palmen, J. (1998). Time-temperature superposition for polymeric blends. *Rheol. Bull.*, 67, 5–8.
- Van der Sman, R. (2019). Phase separation, antiplasticization and moisture sorption in ternary systems containing polysaccharides and polyols. *Food Hydrocolloids*, 87, 360–370.
- van der Sman, R., & Mauer, L. (2019). Starch gelatinization temperature in sugar and polyol solutions explained by hydrogen bond density. *Food Hydrocolloids*, 94, 371–380. <https://doi.org/10.1016/j.foodhyd.2019.03.034>
- Van der Sman, R., & Meinders, M. (2011). Prediction of the state diagram of starch water mixtures using the flory-huggins free volume theory. *Soft Matter*, 7, 429–442.
- Vasanthavada, M., Tong, W.-Q., Joshi, Y., & Kislalioglu, M. S. (2004). Phase behavior of amorphous molecular dispersions i: Determination of the degree and mechanism of solid solubility. *Pharmaceutical Research*, 21, 1598–1606.
- Vergnes, B., Della Valle, G., & Tayeb, J. (1993). A specific slit die rheometer for extruded starchy products. design, validation and application to maize starch. *Rheologica Acta*, 32, 465–476.
- Vergnes, B., & Villemare, J. (1987). Rheological behaviour of low moisture molten maize starch. *Rheologica Acta*, 26, 570–576.
- Wasserman, S., & Graessley, W. (1992). Effects of polydispersity on linear viscoelasticity in entangled polymer melts. *Journal of Rheology*, 36, 543–572.
- Williams, M., Landel, R., & Ferry, J. (1955). The temperature dependence of relaxation mechanisms in amorphous polymers and other glass-forming liquids. *Journal of the American Chemical Society*, 77, 3701–3707.
- Winter, H. H. (1987). Can the gel point of a cross-linking polymer be detected by the g-g crossover? *Polymer Engineering & Science*, 27, 1698–1702.
- Xie, F., Yu, L., Su, B., Liu, P., Wang, J., Liu, H., & Chen, L. (2009). Rheological properties of starches with different amylose/amylopectin ratios. *Journal of Cereal Science*, 49, 371–377.
- You, Y., & Ludescher, R. D. (2007). The effect of glycerol on molecular mobility in amorphous sucrose detected by phosphorescence of erythrosin b. *Food Biophysics*, 2, 133–145.
- Yu, J., & Baird, D. (2019). Study of melt spinning processing conditions for a polyacrylonitrile copolymer with a water/ethanol mixture as a plasticizer. *International Polymer Processing*, 34, 557–563.
- Zhang, C., Shomali, A., Guyer, R., Ketten, S., Coasne, B., Derome, D., & Carmeliet, J. (2020). Disentangling heat and moisture effects on biopolymer mechanics. *Macromolecules*, 53, 1527–1535.
- Zhan, T., Jiang, J., Lu, J., Zhang, Y., & Chang, J. (2019). Frequency-dependent viscoelastic properties of Chinese fir (*Cunninghamia lanceolata*) under hygrothermal conditions. Part 1: Moisture adsorption. *Holzforschung*, 73, 727–736.
- Zorn, R., McKenna, G. B., Willner, L., & Richter, D. (1995). Rheological investigation of polybutadienes having different microstructures over a large temperature range. *Macromolecules*, 28, 8552–8562.